ACI MATERIALS JOURNAL TECHNICAL PAPER

Title no. 104-M20

Piezoresistivity-Based Strain Sensing in Carbon Fiber-Reinforced Cement

by Sihai Wen and D. D. L. Chung

For piezoresistivity-based strain sensing using carbon fiber-reinforced cement (152 mm [6 in.] specimens under compression) in the elastic regime, the four-probe method of electrical resistance measurement is more effective than the two-probe method in that it provides gauge factor (fractional change in resistance per unit strain) that is higher and that varies less with the strain amplitude. The two-probe method also suffers from the resistance increasing irreversibly in the first few loading cycles due to minor degradation of the electrical contacts. The use of embedded stainless steel electrical contacts gives more effective strain sensing and slightly lower resistivity than the use of silver paint surface electrical contacts, whether the four-probe method or the two-probe method is used. In case of the four-probe method, the use of embedded steel contacts compared with the use of surface silver paint contacts results in greater linearity and lower noise in the variation of the resistance with strain. In case of the two-probe method, the use of embedded steel contacts compared with the use of surface silver paint contacts results in lower variability of the gauge factor and smaller fractional contribution of the contact resistance to the measured resistance.

Keywords: carbon; cement; fibers.

INTRODUCTION

Multifunctional cement-based materials are able to provide the structural function (load bearing) plus one or more nonstructural functions. The nonstructural function addressed in this paper is strain sensing.[1-21] Applications of strain (stress) sensing include traffic monitoring (for enhancing safety and mobility of transportation), building evacuation monitoring (that is, determining the room occupancy by weighing each room using smart concrete while the building is being evacuated), border monitoring (that is, monitoring the vehicles and pedestrians in the vicinity of the border through weighing using smart concrete), building security enhancement (that is, detecting an intruder in or around a building by sensing his weight), building facility management (that is, using the room occupancy, as determined by weighing the room, to control the heating, cooling, lighting, and ventilation of a room in real time for the purpose of saving energy), and weighing (such as the weighing of trucks in motion for the purpose of avoiding overweight trucks on highways, the weighing of a truck that is filled with goods before it leaves a factory, and the weighing of cargo in a cargo yard). Damage sensing is valuable for structural health monitoring and hazard mitigation, as needed due to the deterioration of our nation's civil infrastructure, such as bridges, and the need for enhanced homeland security.

A nonstructural function should be attained with little or no compromise on the structural performance. Nonstructural functions such as sensing are conventionally attained in a cement-based material by using embedded or attached devices (for example, strain gauges). This method, however, suffers from the high cost and poor durability of the devices, in addition to the limited functional volume and the tendency for the embedded devices to result in mechanical property loss in the structure. In contrast, this paper addresses the attainment of a nonstructural function without embedded or attached devices, as made possible by special formulation of the cement-based material itself. The formulation involves the use of a minor amount of an admixture for enhancing the function desired. Although the admixture adds to the cost of the cement-based material, its use is less expensive than the use of embedded or attached devices, which are associated with high costs of device acquisition, installation, and maintenance. In particular, the repair of embedded devices is difficult or impossible.

The most effective sensing-enhancing additive for cement-based materials is short carbon fibers (such as those that are 5 mm [0.2 in.] long and 15 μm in diameter).[2] The fibers do not necessarily touch one another. For the purpose of cost reduction, the fiber content should be below the percolation threshold. The percolation threshold is the fiber volume fraction above which the adjacent fibers touch one another, thereby forming a continuous electrically conductive path. The carbon fibers render increased flexural strength, flexural toughness, tensile strength and tensile ductility, and decreased drying shrinkage, in addition to enhanced sensing ability. Thus, the resulting multifunctional cement-based material is attractive from both functional and structural points of view.[4]

The carbon fibers are not the sensor, but are a modifier to the cement-based material. They make the cement-based material strongly piezoresisitive, that is, the electrical resistivity of the cement-based material changing with strain. Upon uniaxial tension, the volume resistivity increases in both the longitudinal and transverse directions;[6] upon uniaxial compression, the volume resistivity decreases in both the longitudinal and transverse directions.[5] Upon flexure (three-point bending), the surface resistance increases at the tension surface and decreases at the compression surface.[21] All of these effects are reversible upon unloading. Furthermore, the piezoresistive effect is strong, with a gauge factor (fractional change in resistance per unit strain) as high as 400. In contrast, the gauge factor is only two for a conventional strain gauge. The piezoresistive effect in this multifunctional cement-based material is due to the slight pull-out of crack-bridging fibers (which are much more conductive than the cement matrix) during crack opening and the consequent

ACI Materials Journal, V. 104, No. 2, March-April 2007.
MS No. M-2006-118 received March 17, 2006, and reviewed under Institute publication policies. Pertinent discussion including authors' closure, if any, will be published in the January-February 2008 *ACI Materials Journal* if the discussion is received by October 1, 2007.

Sihai Wen *is a Postdoctoral Associate, Department of Mechanical and Aerospace Engineering, University at Buffalo, Buffalo, N.Y. He received his PhD in mechanical engineering from the University at Buffalo in 2003.*

D. D. L. Chung *is the National Grid Endowed Chair Professor, Department of Mechanical and Aerospace Engineering, and Director, Composite Materials Research Laboratory, University at Buffalo. She received her PhD in materials science from Massachusetts Institute of Technology, Cambridge, Mass., in 1977.*

increase in the contact electrical resistivity of the fiber-matrix interface.

The addition of carbon fibers allows the sensing of strain (stress) and damage.[17] In general, strain (stress) causes the resistivity to change reversibly while damage (other than very minor damage) causes the resistivity to change irreversibly. The ability to sense both strain (stress) and damage is valuable, as it allows determination of the loading condition at the time of damage infliction, thereby enabling damage cause analysis. In contrast, ultrasonic inspection allows damage condition assessment but not strain (stress) sensing. This paper addresses the strain (stress) sensing, but not the damage sensing. However, the electrical contact configuration evaluation performed in the context of the former is also relevant to the latter.

Strain sensing relates to stress sensing, which in turn relates to weighing. For practical weighing, the accuracy and precision of the weighing need to be sufficient. These attributes of the weighing performance depend on the electrical contact configuration. The quality and durability of the electrical contacts are critical to the implementation of the sensing technology in any application. This paper provides a comparative study of various electrical contact configurations.

The performance of carbon-fiber cement-based materials depends on the degree of dispersion of the fibers in the cement matrix. Good dispersion is particularly important when the fiber content is below the percolation threshold (that is, below the volume fraction necessary for the adjacent fibers to touch one another and form a continuous conductive path). For the sensing function, the fiber volume fraction is preferably below the percolation threshold for the purpose of material cost saving. At the same fiber volume fraction below the percolation threshold, a higher degree of fiber dispersion is associated with a lower electrical resistivity.

Fiber dispersion can be greatly enhanced by the use of appropriate additives. A most effective additive for enhancing the fiber dispersion is silica fume (0.1 μm silica particles, 15% by mass of cement).[22] Fiber surface treatment (surface oxidation) by using ozone also helps the fiber dispersion, because the oxygen-containing functional groups on the surface of the treated fiber help the wettability of the fiber by water.[7,22] Both of these methods of enhancing fiber dispersion are used in this work.

OBJECTIVES

To minimize the effect of the resistance associated with the electrical contacts, the four-probe method is preferred to the two-probe method for the purpose of accurate sensing. In the four-probe method, the outer two probes are for passing current, whereas the inner two probes are for voltage measurement. In contrast, in the two-probe method, each of the two probes is both for current application and voltage measurement. As a consequence, the measured resistance based on the two-probe method includes the contact resistance. Both the four-probe method[1,3,5-11,14,17-21,23,24] and the two-probe method[12,13,25-30] have been used in prior work on carbon fiber-reinforced cement.

The contact resistance is associated with the resistance of the interface between the electrical contact and the specimen surface and the resistance within the contact material. The electrical contact materials are electronic conductors rather than ionic conductors because electrical conduction in carbon fiber-reinforced cement is mainly electronic rather than ionic.[31] Because the electrical contact material is a good electrical conductor (for example, metals such as silver, copper, and steel), the contact resistance is mainly associated with the resistance of the interface. On the other hand, the two-probe method is more suitable than the four-probe method for practical implementation in structures. Therefore, it is important to evaluate the two methods comparatively and, in addition, determine the effectiveness of the two-probe method (in spite of its known drawback). This is the first objective of this paper.

The greater the resistance of the specimen, the less important is the contact resistance contribution. The multifunctional cement-based material of this work is cement containing carbon fibers at a volume fraction below the percolation threshold. As a consequence, the electrical resistivity of the material is quite high (1.5×10^4 Ω·cm).[11] This value is only an order of magnitude less than that of plain cement (that is, cement with no conductive admixture). Due to the high resistance of a specimen, the resistance measured by using the two-probe method can be sufficiently accurate, as shown in this paper.

The electrical contacts for a cement-based material can be embedded in the cement-based material, either during the fabrication of the material or afterward, by screwing in an electrical contact in the form of a steel rivet. Alternatively, they can be applied on the surface of the cement-based material after the fabrication of the material. The advantage of the former pertains to greater mechanical integrity, which means greater durability, although the screwing in of a rivet is intrusive. The advantage of the latter lies on the applicability to existing structures without intrusion. Thus, it is important to develop both types of electrical contacts and evaluate their effectiveness. Such an evaluation is the second objective of this paper.

In case of the two-probe method, the electrical contacts that are on the surface of a cement-based structural column, for example, can be applied parametrically around the column in a plane that is perpendicular to the axis of the column. Alternatively, they can be at the top and bottom end surfaces of the column, as in the case of having the top contact between a column and a precast slab above and having the bottom contact between the column and a precast slab below. The latter configuration is advantageous in the difficulty of the contacts coming off, but it is disadvantageous in that the contacts are compressed along the axis of the column during operation and that this compression may affect the quality of the contacts. The former configuration is advantageous in that the contacts are not compressed during operation, but is disadvantageous in that the contacts are more prone to becoming loose or damaged. Thus, it is important for both configurations to be evaluated. Such an evaluation is the third objective of this paper.

The comparative electrical contact evaluation of this paper includes: 1) comparison of the four-probe and two-probe methods for each contact style; 2) comparison of surface electrical contacts and embedded contacts in both four-probe and two-probe methods; and 3) comparison of parametric surface contacts and end surface contacts in the two-probe method.

The overall objective of this paper is to compare the effectiveness of various electrical contact configurations for piezoresistivity-based strain sensing in carbon fiber-reinforced cement. Although various contact configurations have been used in prior work, there has been no prior report that compares the effectiveness of the various configurations. Finding out the strengths and weaknesses of the various configurations is valuable for scientific research as well as practical implementation of the sensing technology.

RESEARCH SIGNIFICANCE

This paper provides basic data associated with the effectiveness of various electrical contact configurations for conducting piezoresistivity-based strain sensing using carbon fiber-reinforced cement. The data relate to the sensitivity, accuracy, and repeatability of the strain sensing.

EXPERIMENTAL METHODS

Materials

The cement-based material used in the study is carbon fiber-reinforced cement paste. In other words, there is no aggregate. The paste contains ozone-treated carbon fiber and silica fume.

The carbon fiber is isotropic pitch-based, unsized, and has a diameter of 15 μm and nominal length of 5 mm (0.2 in.). Fibers are in the amount of 0.5% by mass of cement (corresponding to 0.5 vol.%).

The ozone treatment of the fibers, as conducted prior to incorporating the fibers in the cement mixture, involves drying the fibers at 110 °C (230 °F) in air for 1 hour and then surface treating with ozone by exposure to ozone gas (0.6 vol.% in oxygen) at 160 °C (320 °F) for 10 minutes.

The cement is portland cement (Type I). The water-cement ratio is 0.35. No aggregate is used. A water-reducing agent is used in the amount of 1.0% by mass of cement.

The silica fume is in the amount of 15% by mass of cement. The methylcellulose is in the amount of 0.4% by mass of cement and is used along with the silica fume. The defoamer is in the amount of 0.13 vol.% (percent of specimen volume) and is used along with the methylcellulose.

A rotary mixer with a flat beater is used for mixing. Methylcellulose is dissolved in water and then the defoamer is added and stirred by hand for approximately 2 minutes. Then the methylcellulose solution, cement, water, silica fume, and fibers are mixed in the mixer for 5 minutes. After pouring into molds, an external vibrator is used to facilitate compaction and decrease the amount of air bubbles. The specimens are demolded after 24 hours and then cured in air at room temperature and a relative humidity of 100% for 28 days.

Testing

The piezoresistivity-based strain sensing evaluated in this work in one dimension relates to application of the technology to columns. The specimen is in the form of a 6 in. column with a square (2 x 2 in. [51 x 51 mm]) cross section (Fig. 1). Compressive stress is applied along the axis of the column. Electrical contacts are applied to the column for the purpose of electrical resistance measurement. The DC electrical resistance is continuously measured using a multimeter, while compressive loading at various strain amplitudes is repeatedly applied along the length of the specimen using a hydraulic mechanical testing system. The loading is all within the elastic regime. The strain in the longitudinal direction is measured by using an adhesively-attached metallic strain gauge. Reliability of the strain measurement is shown by measurement of three specimens of each type and indication of the data scatter in Tables 1 and 2.

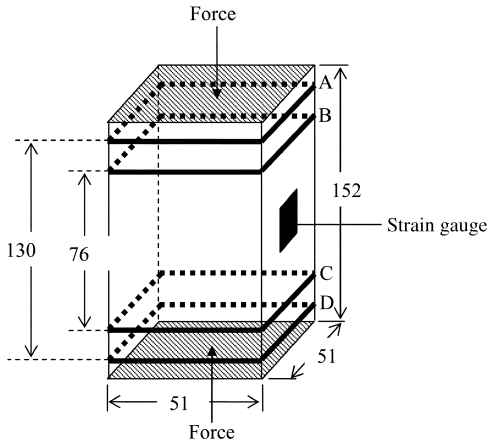

Fig. 1—Specimen configuration for testing sensing performance in one dimension. Four-probe Method B is illustrated. Four electrical contacts are A, B, C, and D. All dimensions are in mm. (Note: 1 mm = 0.039 in.)

Five electrical contact configurations are evaluated in this work, as listed in the following.

1. Four-probe Method A, in which the four electrical contacts are in the form of embedded stainless steel foil.
2. Four-probe Method B, in which the four electrical contacts are in the form of silver paint in conjunction with copper wire parametrically on the surface.
3. Two-probe Method A, in which the two electrical contacts are in the form of embedded stainless steel foil, that is, the inner two of the four contacts in four-probe Method A.
4. Two-probe Method B, in which the two electrical contacts are in the form of silver paint in conjunction with copper wire parametrically on the surface, that is, the inner two of the four contacts in four-probe Method B.
5. Two-probe Method C, in which the two electrical contacts are in the form of silver paint in conjunction with copper foil on the surface if the two ends that are perpendicular to the stress direction. For each contact, silver paint is applied between the specimen surface and the copper foil. During compression of the specimen, each contact is necessarily compressed in the direction perpendicular to the plane of the contact.

For each contact configuration, evaluation is conducted in terms of the measured electrical resistivity, the gauge factor (the fractional change in resistance per unit strain, that is, a measure of the strain sensitivity), the data scatter (as shown by testing three specimens of each type), and the possible effect of strain history.

The electrical contacts used successfully in previous work are mainly in the form of parametric surface contacts, such as those made by using silver paint in conjunction with copper wire. The use of embedded contacts (such as embedded steel) has received less prior attention. Although copper is more conductive than steel, copper suffers from surface oxidation and reaction in the presence of moisture. Steel is commonly used in cement-based materials for reinforcement anyway. Stainless steel is even more attractive, due to its corrosion resistance. Thus, the use of embedded stainless steel electrical contacts is evaluated in this work, with comparison made with the use of parametric silver paint

surface contacts. In each case, both the four-probe and two-probe methods are used. The inner contacts are 76 mm (3 in.) apart from one another. The outer contacts are 130 mm (5 in.) apart from one another, such that each contact is at a distance of 13 mm (0.5 in.) from an end of the column. Hence, the adjacent current and voltage contacts are 25 mm (1 in.) apart.

A silver paint surface contact is installed by applying silver paint in conjunction with copper wire around the whole perimeter of the column after the column has been cured and dried. Because silver paint is the medium between the cement-based specimen surface and the copper wire, silver paint rather than copper is the actual electrical contact material. The silver paint is in the form of fine silver particles dispersed in a volatile liquid vehicle that contains a small amount of a binder. It is in the form of a paste of low viscosity. Because of the low viscosity, silver paint can flow and fill the small gap between the specimen surface and the copper wire. After application, the silver paint is allowed to dry in air. The drying process takes 1 day.

An embedded stainless steel contact is installed in the column during the pouring of the cement to form the column. In this work, each steel contact is in the form of a stainless steel foil (0.06 mm [0.0023 in.] thick) that has punched holes of a diameter of 3 mm (0.12 in.), such that the edges of adjacent holes are spaced apart by a distance ranging from 2 to 3 mm (0.08 to 0.12 in.) and the holes are arranged in a square array and they occupy 17.4% of the 50 x 50 mm (2 x 2 in.) embedded foil area. The holes allow mechanical interlocking between the foil and the cement. The embedded steel foil is as large as the cross section of the specimen to ensure uniform current injection. In practical application, however, the embedded steel foil can be smaller than the cross section of the column.

RESULTS AND DISCUSSION

Figures 2 and 3 show the fractional change in longitudinal resistance during repeated loading at various strain amplitudes for four-probe Methods A and B, respectively. The series of strain amplitudes used in the 10 cycles, as designed to investigate if there is any effect of the strain history, is the same for all of the five contact configurations evaluated. The strain is returned to zero at the end of each stress cycle. Examination of the fractional change in resistance for the series of stress cycles in Fig. 2 and 3 shows that there is no dependence on the strain history, as explained in the following. Cycles 1, 3, and 10 have essentially the same strain amplitude of -0.27×10^{-4}; Cycles 2 and 5 have essentially the same strain amplitude of

Table 1—Strain amplitude and corresponding gauge factor for each cycle of uniaxial compression imposed on carbon fiber cement*

	Strain amplitude (10^{-4})		Gauge factor		Resistivity (10^4 Ω·cm)	
Cycle no.	B†	A†	B†	A†	B†	A†
1	–0.284 ± 0.02	–0.27 ± 0.01	313 ± 40	287 ± 42	1.30 ± 0.16	1.20 ± 0.16
2	–0.576 ± 0.03	–0.52 ± 0.03	258 ± 37	285 ± 40	1.29 ± 0.15	1.19 ± 0.14
3	–0.284 ± 0.02	–0.27 ± 0.01	308 ± 46	286 ± 37	1.30 ± 0.17	1.20 ± 0.16
4	–0.805 ± 0.04	–0.82 ± 0.03	242 ± 31	278 ± 46	1.29 ± 0.18	1.18 ± 0.17
5	–0.584 ± 0.02	–0.55 ± 0.02	235 ± 27	291 ± 41	1.30 ± 0.14	1.19 ± 0.14
6	–1.13 ± 0.04	–1.13 ± 0.04	219 ± 28	267 ± 33	1.28 ± 0.17	1.17 ± 0.15
7	–0.806 ± 0.04	–0.87 ± 0.03	238 ± 30	286 ± 43	1.29 ± 0.16	1.18 ± 0.14
8	–1.42 ± 0.03	–1.45 ± 0.03	211 ± 26	278 ± 45	1.27 ± 0.14	1.15 ± 0.14
9	–1.13 ± 0.05	–1.17 ± 0.04	214 ± 29	285 ± 35	1.28 ± 0.15	1.17 ± 0.13
10	–0.28 ± 0.02	–0.28 ± 0.01	275 ± 43	278 ± 39	1.30 ± 0.18	1.20 ± 0.18

*With silver paint surface electrical contacts (four-probe Method B) and embedded in steel electrical contacts (four-probe Method A). Initial resistivity is $(1.22 \pm 0.18) \times 10^4$ Ω·cm and $(1.32 \pm 0.20) \times 10^4$ Ω·cm for four-probe Methods A and B, respectively. Three specimens for each type were tested.
†Four-probe method designation.

Table 2—Strain amplitude and corresponding gauge factor for each cycle of uniaxial compression imposed on carbon fiber cement*

	Strain amplitude (10^{-4})			Gauge factor			Resistivity (10^4 Ω·cm)		
Cycle no.	C†	B†	A†	C†	B†	A†	C†	B†	A†
1	–0.27± 0.02	–0.27± 0.03	–0.27 ± 0.02	270 ± 33	243 ± 28	239 ± 27	1.452 ± 0.183	1.510 ± 0.204	1.331 ± 0.148
2	–0.52 ± 0.04	–0.54± 0.04	–0.51± 0.03	171 ± 28	137 ± 20	174 ± 23	1.455 ± 0.176	1.513± 0.206	1.334 ± 0.163
3	–0.27± 0.02	–0.26± 0.03	–0.26 ± 0.02	226 ± 35	198 ± 32	212 ± 35	1.465 ± 0.168	1.521 ± 0.194	1.339 ± 0.162
4	–0.81 ± 0.04	–0.79 ± 0.03	–0.79 ± 0.02	102 ± 17	94 ± 15	115 ± 14	1.463 ± 0.175	1.520 ± 0.222	1.336 ± 0.189
5	–0.54± 0.03	–0.53± 0.02	–0.53 ± 0.03	137 ± 18	122 ± 18	166 ± 19	1.467 ± 0.154	1.525 ± 0.235	1.337 ± 0.168
6	–1.09 ± 0.03	–1.05 ± 0.02	–1.07 ± 0.02	85 ± 14	70 ± 11	93 ± 13	1.466 ± 0.192	1.526 ± 0.233	1.336 ± 0.181
7	–0.81± 0.04	–0.82 ± 0.03	–0.80 ± 0.02	92 ± 15	81 ± 13	110 ± 14	1.468 ± 0.188	1.527 ± 0.217	1.337 ± 0.154
8	–1.39 ± 0.03	–1.32 ± 0.02	–1.35 ± 0.02	67 ± 12	60 ± 10	98 ± 12	1.466 ± 0.201	1.526 ± 0.251	1.336 ± 0.203
9	–1.15 ± 0.04	–1.05 ± 0.03	–1.08 ± 0.02	73 ± 11	66 ± 11	89 ± 13	1.468 ± 0.177	1.527 ± 0.234	1.337 ± 0.182
10	–0.28 ± 0.02	–0.26 ± 0.02	–0.26 ± 0.02	162 ± 27	160 ± 27	191 ± 26	1.471 ± 0.163	1.530 ± 0.209	1.334 ± 0.174

*With two electrical contacts. Initial resistivity is $(1.46 \pm 0.22) \times 10^4$ Ω·cm for two-probe Method C, $(1.53 \pm 0.26) \times 10^4$ Ω·cm for two-probe Method B, and $(1.34 \pm 0.19) \times 10^4$ Ω·cm for two-probe Method A.
†Two-probe method designation, as explained in Experimental Methods section.

-0.52×10^{-4}; Cycles 4 and 7 have essentially the same strain amplitude of -0.85×10^{-4}; and Cycles 6 and 9 have essentially the same strain amplitude of -1.1×10^{-4}. In spite of the difference in strain history among the cycles in each of these groups, different cycles at essentially the same strain amplitude give essentially the same fractional change in resistance. The absence of strain history dependence adds to the feasibility of strain sensing using this multifunctional cement-based material.

The initial resistivity (prior to any loading) is $(1.22 \pm 0.18) \times 10^4$ Ω·cm and $(1.32 \pm 0.20) \times 10^4$ Ω·cm for four-probe Methods A and B, respectively. Three specimens of each type were tested. The data scatter is shown along with the average value for the initial resistivity values (as mentioned previously) as well as the resistivity at the maximum strain of each cycle (Table 1). That the initial resistivity values for four-probe Methods A and B are essentially equal indicates the validity of both electrical contact technologies. Although the initial resistivity values are similar, the resistivity is slightly lower for four-probe Method A than for four-probe Method B. This means that the embedded steel contacts provide slightly more uniform current distribution throughout the cross section of the specimen than the surface silver paint contacts, thereby resulting in a slightly lower measured resistivity. This result is consistent with that indicated by finite element modeling, which is the subject of a separate paper.[32] Table 1 shows similarity of the resistivity at the maximum strain of each cycle for four-probe Methods A and B. Hence, the similarity in the resistivity values between four-probe Methods A and B occurs both before loading and during repeated loading at various strain amplitudes.

Comparison of Fig. 2 and 3 shows that the signal-to-noise ratio is higher for four-probe Method A than four-probe Method B. This is probably due to the greater mechanical stability of the embedded contacts than the surface contacts during repeated loading. The greater signal-to-noise level, along with the greater current density uniformity mentioned previously, for four-probe Method A compared with four-probe Method B, makes the former practically attractive. In practical implementation, the stainless steel foils (with punched holes occupying only 17.4% of the embedded area) may be replaced by a stainless steel wire mesh, so that the aggregates in the mixture can easily pass through the contact material during fabrication. The mesh size should be such that the holes in the mesh are larger than the coarse aggregate in the mixture.

Table 1 shows the similarity of the gauge factor (fractional change in resistance per unit strain) for four-probe Methods A and B. This means that both methods are effective for attaining strain sensing. The gauge factor has a scatter of up to 16% among the three specimens of each type tested. In real structural application, this variability in the gauge factor is less of an issue because a particular structure is always a particular piece of cement-based material (unless the structure is dismantled) and the strain sensing calibration is conducted for that particular piece of material. In spite of the similarity, the gauge factor has more variability among the cycles for four-probe Method B (gauge factor ranging from 211 to 313, that is, 48% variation) than four-probe Method A (gauge factor ranging from 267 to 291, that is, 9% variation). The lower variability of the gauge factor for four-probe Method A compared with four-probe Method B is consistent with the slightly lower resistivity for four-probe Method A. Thus,

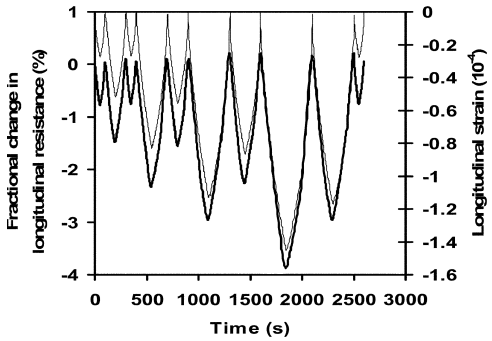

Fig. 2—Curves of fractional change in longitudinal resistance (thick curve) versus time and of longitudinal strain (thin curve) versus time using repeated compression at various strain amplitudes, for four-probe Method A.

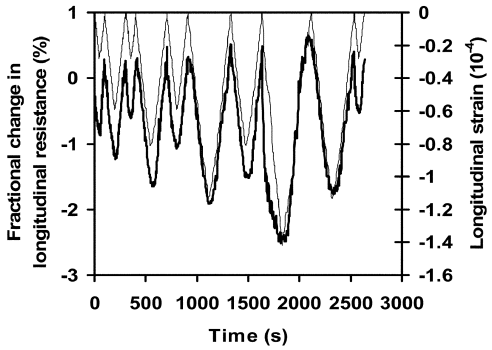

Fig. 3—Curves of fractional change in longitudinal resistance (thick curve) versus time and of longitudinal strain (thin curve) versus time using repeated compression at various strain amplitudes, for four-probe Method B.

four-probe Method A is superior to four-probe Method B for strain sensing.

Figures 4 through 6 give results obtained using two-probe Methods A, B, and C, respectively.

The measured resistivity values for two-probe Method A (Table 2) are higher than those obtained using four-probe Method A (Table 1); the measured resistivity values for two-probe Method B (Table 2) are higher than those obtained using four-probe Method B (Table 1). This is expected due to the inclusion of the contact resistance in the measured resistance obtained using the two-probe method. The measured resistivity for two-probe Method C is slightly lower than that for two-probe Method B, but is slightly higher than that for two-probe Method A. This means that the current density uniformity is superior for two-probe Method C than two-probe Method B, but is inferior for two-probe Method C than two-probe Method A.

In spite of the differences in resistivity among the five methods, all the differences are small. In particular, the difference in resistivity measured by using four-probe Method A and two-probe Method A indicates that the contact resistance contributes to 9% of the resistance measured by using two-probe Method A; the difference in resistivity measured by using four-probe Method B and two-probe Method B indicates that the contact resistance contributes to 14% of the resistance measured by using two-probe Method B. The lower fractional contribution of the contact resistance in two-probe Method A compared with two-probe Method B is consistent with the lower variability of the

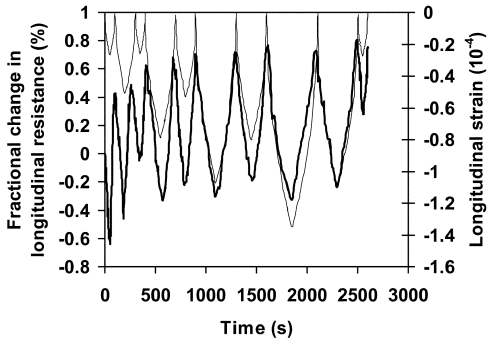

Fig. 4—Curves of fractional change in longitudinal resistance (thick curve) versus time and of longitudinal strain (thin curve) versus time using repeated compression at various strain amplitudes, for two-probe Method A.

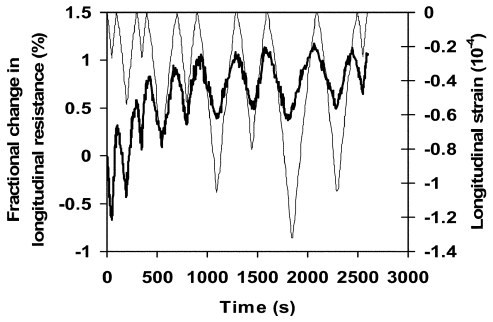

Fig. 5—Curves of fractional change in longitudinal resistance (thick curve) versus time and of longitudinal strain (thin curve) versus time using repeated compression at various strain amplitudes, for two-probe Method B.

gauge factor among the cycles for two-probe Method A (gauge factor ranging from 89 to 239, that is, 170% variation) than two-probe Method B (gauge factor ranging from 60 to 243, that is, 310% variation). Thus, two-probe Method A is superior to two-probe Method B.

The gauge factor varies from 267 to 291 (9% variation) among the cycles for four-probe Method A (Table 1), but varies from 89 to 239 (170% variation) for two-probe Method A (Table 2). Hence, the gauge factor is higher and its variability is lower for four-probe Method A than two-probe Method A. For accurate sensing of strain/stress, a high gauge factor is desirable. For precise sensing of strain/stress, a small variability of the gauge factor is desirable. Therefore, although strain/stress sensing is feasible using two-probe Method A, the accuracy and precision of the sensing are better for four-probe Method A than two-probe Method A.

The gauge factor varies from 211 to 313 (48% variation) among the cycles for four-probe Method B (Table 1), and varies from 60 to 243 (310% variation) for two-probe Method B (Table 2). Hence, the gauge factor is higher and its variability is lower for four-probe Method B than two-probe Method B. Thus, the accuracy and precision of the sensing are better for four-probe Method B than two-probe Method B.

The gauge factor varies from 67 to 270 (300% variation) for two-probe Method C, and from 60 to 243 (310% variation) for two-probe Method B. Thus, these two methods give similar values and variability of the gauge factor.

In two-probe Method C, the compressive loading is directly applied on the electrical contacts, which are at the two ends of the specimen. Thus, one may expect that two-probe Method C would be particularly susceptible to contact quality change during loading. One may expect the contact quality to improve upon compression of the contact material on the specimen surface. One may alternatively expect the contact quality to degrade upon compression due to the degradation of the dried silver paint upon compression. This work shows that the contacts in two-probe Method C are degraded rather than improved upon compression, as shown by the irreversible increase of the resistivity during the first few loading cycles (Fig. 6).

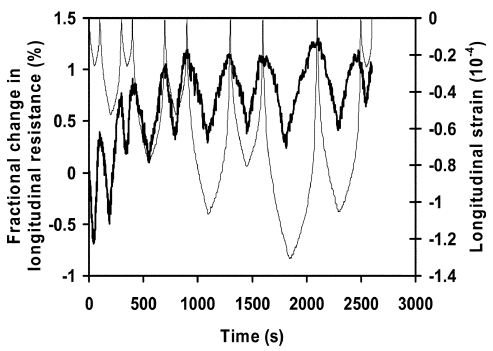

Fig. 6—Curves of fractional change in longitudinal resistance (thick curve) versus time and of longitudinal strain (thin curve) versus time using repeated compression at various strain amplitudes, for two-probe Method C.

The contact degradation is minor and cannot be visually observed. That the degradation is minor is supported by the small fractional increase in the measured two-probe resistivity during the first three cycles (Fig. 4 through 6). The fractional increase is 0.6, 0.7. and 0.9% for two-probe Methods A, B, and C, respectively (Table 2). Two-probe Methods A, B, and C (Fig. 4 through 6, respectively) are all susceptible to minor degradation of the contact quality during loading, but two-probe Method A is probably less susceptible than two-probe Method B, which is, in turn, probably less susceptible than two-probe Method C. The relative susceptibility for contact degradation among two-probe Methods A, B, and C is not totally clear, due to the data scatter.

Although the increase in contact resistance due to contact degradation in two-probe Methods A, B, and C is small (0.9% or less) and the contribution of the contact resistance to the measured two-probe resistance is small (as low as 9%), the gauge factor is much lower for the two-probe method than the corresponding four-probe method (Tables 1 and 2 in comparison). The low values of the gauge factor in case of the two-probe method are attributed to the change of the contact resistivity during dynamic loading contributing significantly to the observed piezoresistivity. In other words, the increase in contact resistance opposes the decrease in volume resistance during compression, thereby diminishing the gauge factor.

Tables 1 and 2 show the resistivity at the peak strain averaged over the three specimens of each electrical contact configuration. To investigate the dependence of the resistivity at the peak strain with the strain amplitude, it is better to consider this variation for a single specimen rather than considering the variation of the average resistivity of three specimens. This is because the variation among specimens overshadows the variation with the strain amplitude. In practical implementation, the structure is always one particular piece of material, unless it is dismantled and replaced. Therefore, it is valuable

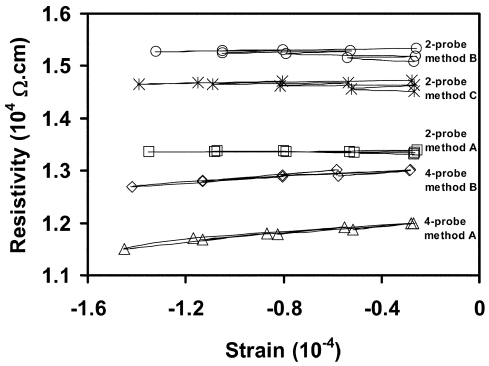

Fig. 7—Variation of resistivity at peak strain versus strain amplitude for single specimen of each of five electrical contact configurations. Data correspond to those of Fig. 2 though 6.

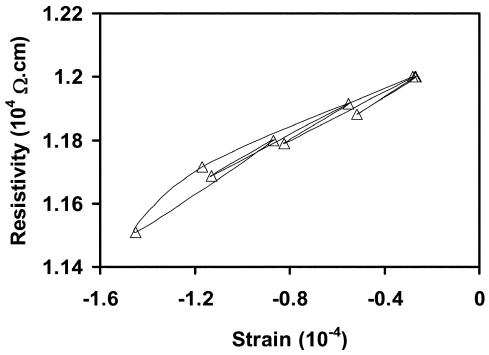

Fig. 8—Magnified view of Fig. 7 for four-probe Method A. Data points are connected with line drawn to indicate order in which various strain amplitudes are imposed. Order is as shown in Fig. 2. Data correspond to those of Fig. 2.

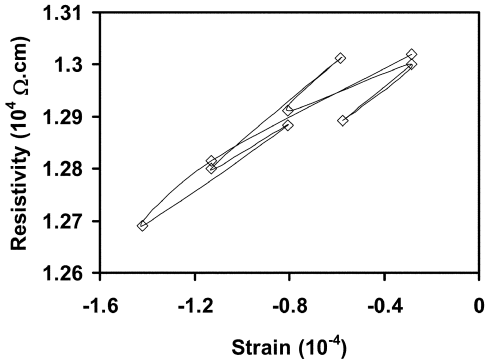

Fig. 9—Magnified view of Fig. 7 for four-probe Method B. Data points are connected with line drawn to indicate order in which various strain amplitudes are imposed. Order is shown in Fig. 3. Data correspond to those of Fig. 3.

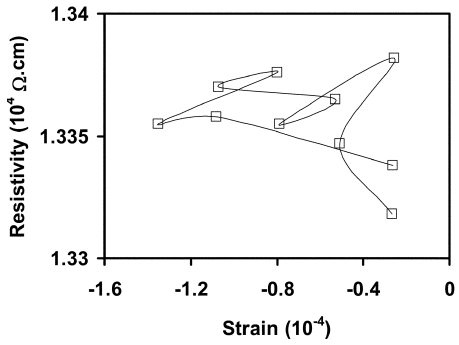

Fig. 10—Magnified view of Fig. 7 for two-probe Method A. Data points are connected with line drawn to indicate order in which various strain amplitudes are imposed. Order is as shown in Fig. 4. Data correspond to those of Fig. 4.

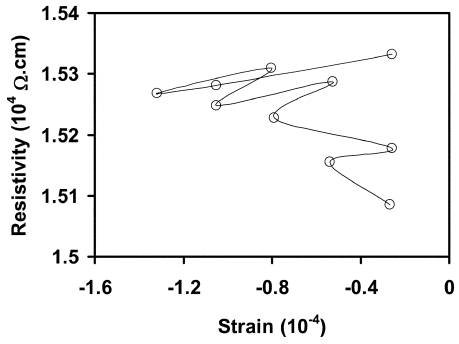

Fig. 11—Magnified view of Fig. 7 for two-probe Method B. Data points are connected with line drawn to indicate order in which various strain amplitudes are imposed. Order is as shown in Fig. 5. Data correspond to those of Fig. 5.

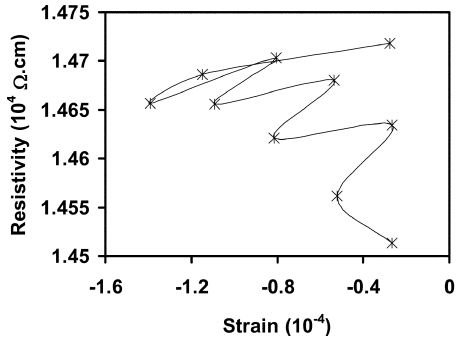

Fig. 12—Magnified view of Fig. 7 for two-probe Method C. Data points are connected with line drawn to indicate order in which various strain amplitudes are imposed. Order is as shown in Fig. 6. Data correspond to those of Fig. 6.

to consider the variation of a single specimen. Figure 7 shows the variation for a single specimen of each configuration.

The resistivity at the peak strain decreases monotonically with increasing magnitude of the strain amplitude for four-probe Methods A and B, as shown in a magnified view in Fig. 8 and 9, respectively. However, it varies little with the strain amplitude for two-probe Methods A, B, and C. This is consistent with the large values of the gauge factor for four-probe Methods A and B than for two-probe Methods A, B, and C. Comparison of Fig. 8 and 9 shows that the resistivity has less strain history dependence for four-probe Method A than four-probe Method B. Both methods give a roughly linear relationship between the resistivity at the peak strain and the strain amplitude. The linear behavior means that the gauge factor is independent of the strain amplitude. It is attractive for strain sensing. The degree of linearity is higher for four-probe Method A than four-probe Method B.

Two-probe Methods A, B, and C do not show any systematic dependence of the resistivity at the peak strain on the strain amplitude, as shown in Fig. 10 through 12, respectively, although the variation is small (Fig. 7). The nonsystematic dependence partly reflects the irreversible increase in resistivity

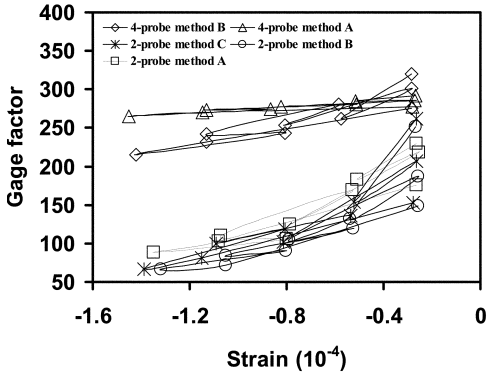

Fig. 13—Effect of strain amplitude on gauge factor, as shown for one specimen of each electrical contact configuration. Data correspond to those of Fig. 2 though 6.

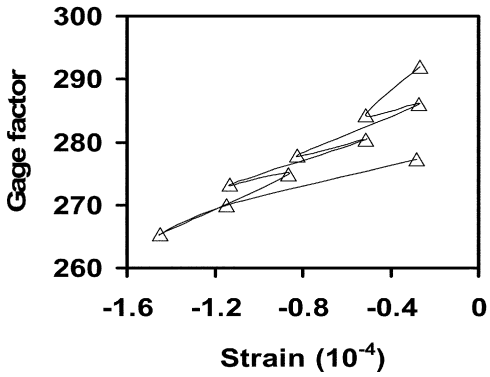

Fig. 14—Effect of strain amplitude on gauge factor, as shown for one specimen of four-probe Method A. Data points are connected with line drawn to indicate order in which various strain amplitudes are imposed. Order is as shown in Fig. 2. Data correspond to those in Fig. 2.

during the first few cycles. This irreversible increase is particularly significant for two-probe Methods B and C, as shown in Fig. 11 and 12, respectively. The nonsystematic dependence of the resistivity at the peak strain on the strain amplitude is consistent with the large variability in the gauge factor among the cycles, as discussed previously.

Tables 1 and 2 show essentially no systematic effect of the strain amplitude on the gauge factor. It is better to study the effect in a single specimen, however, rather than considering the average value of the gauge factor for three specimens of each electrical contact configuration. As shown in Fig. 13, for one specimen of each electrical contact configuration, the gauge factor is essentially independent of the strain amplitude for four-probe Method A, but decreases with increasing magnitude of the strain amplitude for four-probe Method B and for two-probe Methods A, B, and C. Figure 14 (a magnified view of Fig. 13 for four-probe Method A) shows that the gauge factor decreases slightly with increasing magnitude of the strain amplitude, even for four-probe Method A. This effect of the strain amplitude on the gauge factor limits the accuracy of strain sensing. The greater the percentage variation of the gauge factor, the lower the accuracy. As shown in Fig. 13, the accuracy is highest for four-probe Method A, less for four-probe Method B, and least for two-probe Methods A, B, and C.

In summary, the gauge factor is lower and varies more with the strain amplitude for two-probe Methods A, B, and C (Table 2) than for four-probe Methods A and B (Table 1). Moreover, the variation of the resistance with strain is less noisy, the gauge factor is higher, and the gauge factor variability is less for four-probe Method A (Fig. 2 and Table 1) than two-probe Method A (Fig. 4 and Table 2). Similarly, the gauge factor is higher and the gauge factor variability is less for four-probe Method B than two-probe Method B, but the noise level is similar for these two methods. Four-probe Method A is superior to four-probe Method B in the lower noise and the lower variability of the gauge factor. Two-probe Method A is superior to two-probe Method B in the smaller fractional contribution of the contact resistance to the measured resistance and in the lower variability of the gauge factor. The resistance obtained using two-probe Methods A, B, and C increases irreversibly in the first few cycles (Fig. 4 through 6), due to minor degradation of the electrical contacts during the cycling. This does not occur for four-probe Method A or B (Fig. 2 and 3).

The aforementioned findings have the following practical implications. First, among the five methods evaluated, four-probe Method A is the best for providing accurate and precise sensing. Second, two-probe Method A provides sensing, though the accuracy and precision are lower than those provided by four-probe Method A and it suffers from higher noise and from the resistance increasing irreversibly during the first few cycles of loading. Third, the use of embedded steel contacts is considerably more effective than the use of surface silver paint contacts in case of the four-probe method, but is only slightly more effective than the use of surface silver paint contacts in case of the two-probe method.

For a column of length L and cross-sectional area A, the volume resistance R_v is given by $\rho_v L/A$, where ρ_v is the volume electrical resistivity of the material of the column. Consider the configuration of two-probe Method A or C. The contact resistance R_c of each of the electrical contacts is given by ρ_c/A, where ρ_c is the contact resistivity of the electrical contact. The ratio of R_c to R_v is independent of A and is equal to $\rho_c/\rho_v L$. Hence, the larger L is, the less important R_c is relative to R_v.

In two-probe Method A, where L = 76 mm (3 in.) (Fig. 5), the contact resistance amounts to 9% of the two-probe resistance. Thus, the ratio of the contact resistance to the volume resistance is 10%. If L is 7600 mm (7.6 m [25 ft]), this ratio will be 0.1%. Therefore, the contact resistance contribution is much smaller for real structures than laboratory specimens. This means that the effectiveness of the two-probe method is expected to be much greater for real structures than laboratory specimens. For real structures, the two-probe method may provide adequate strain sensing. For small laboratory specimens, however, as shown by the aforementioned results, the two-probe method has limitations.

CONCLUSIONS

For piezoresistivity-based strain sensing using carbon fiber-reinforced cement (152 mm [6 in.] specimens under compression) in the elastic regime, the four-probe method is more effective than the two-probe method in that it provides a gauge factor that is higher and that varies less with the strain amplitude (that is, greater linearity of the curve of the resistivity at the peak strain versus the strain amplitude), thereby allowing more accurate strain sensing. The two-probe method also suffers from the resistance increasing irreversibly by up to 0.9% in the first few loading cycles due to minor degradation of the electrical contacts. The use of

embedded stainless steel electrical contacts gives more effective strain sensing and slightly lower resistivity than the use of silver paint surface electrical contacts, whether the four-probe method or the two-probe method is used. In case of the four-probe method, the use of embedded steel contacts compared with the use of surface silver paint contacts results in greater linearity (gauge factor variation of 9% rather than 48%) and lower noise in the variation of the resistance with strain. In case of the two-probe method, the use of embedded steel contacts compared with the use of surface silver paint contacts results in lower variability of the gauge factor and smaller fractional contribution of the contact resistance to the measured resistance (9% rather than 14%). The two-probe method involving copper foil electrical contacts at the specimen ends (where loading is applied) gives results that are similar to the two-probe method involving surface silver paint contacts that are parametrically around the specimen.

ACKNOWLEDGMENTS

This work was supported in part by the U.S. Army. It was a part of an SBIR project directed by J. H. Chung of Global Contour Ltd.

REFERENCES

1. Chen, P.-W., and Chung, D. D. L., "Concrete as a New Strain/Stress Sensor," *Composites*, Part B, V. 27, 1996, pp. 11-23.

2. Chung, D. D. L., "Piezoresistive Cement-Based Materials for Strain Sensing," *Journal of Intelligent Materials Systems and Structures*, V. 13, No. 9, pp. 599-609.

3. Wen, S., and Chung, D. D. L., "A Comparative Study of Steel- and Carbon-Fibre Cement as Piezoresistive Strain Sensors," *Advances in Cement Research*, V. 15, No. 3, 2003, pp. 119-128.

4. Chung, D. D. L., "Electrical Conduction Behavior of Cement-Matrix Composites," *Journal of Materials Engineering and Performance*, V. 11, No. 2, 2002, pp. 194-204.

5. Wen, S., and Chung, D. D. L., "Uniaxial Compression in Carbon Fiber Reinforced Cement, Sensed by Electrical Resistivity Measurement in Longitudinal and Transverse Directions," *Cement and Concrete Research*, V. 31, No. 2, 2001, pp. 297-301.

6. Wen, S., and Chung, D. D. L., "Uniaxial Tension in Carbon Fiber Reinforced Cement, Sensed by Electrical Resistivity Measurement in Longitudinal and Transverse Directions," *Cement and Concrete Research*, V. 30, No. 8, 2000, pp. 1289-1294.

7. Fu, X.; Lu, W.; and Chung, D. D. L., "Ozone Treatment of Carbon Fiber for Reinforcing Cement," *Carbon*, V. 36, No. 9, 1998, pp. 1337-1345.

8. Fu, X., and Chung, D. D. L., "Effect of Curing Age on the Self-Monitoring Behavior of Carbon Fiber Reinforced Mortar," *Cement and Concrete Research*, V. 27, No. 9, 1997, pp. 1313-1318.

9. Chen, P.-W., and Chung, D. D. L., "Carbon Fiber Reinforced Concrete as a Smart Material Capable of Non-Destructive Flaw Detection," *Smart Materials and Structures*, V. 2, 1993, pp. 22-30.

10. Wen, S., and Chung, D. D. L., "Carbon Fiber-Reinforced Cement as a Strain-Sensing Coating," *Cement and Concrete Research*, V. 31, No. 4, 2001, pp. 665-667.

11. Wen, S., and Chung, D. D. L., "Strain-Sensing Characteristics of Carbon Fiber-Reinforced Cement," *ACI Materials Journal*, V. 102, No. 4, July-Aug. 2005, pp. 244-248.

12. Sun, M.; Mao, Q.; and Li, Z., "Size Effect and Loading Rate Dependence of the Pressure-Sensitivity of Carbon Fiber Reinforced Concrete (CFRC)," *Journal of Wuhan University of Technology*, Materials Science Edition, V. 13, No. 3, 1998, pp. 58-61.

13. Mao, Q.; Zhao, B.; Sheng, D.; and Li, Z., "Resistance Changement of Compression Sensible Cement Specimen Under Different Stresses," *Journal of Wuhan University of Technology*, Materials Science Edition, V. 11, No. 3, 1996, pp. 41-45.

14. Reza, F.; Batson, G. B.; Yamamuro, J. A.; and Lee, J. S., "Resistance Changes During Compression of Carbon Fiber Cement Composites," *Journal of Materials for Civil Engineering*, V. 15, No. 5, 2003, pp. 476-483.

15. Wu, Y.; Bing, C.; and Keru, W., "Smart Characteristics of Cement-Based Materials Containing Carbon Fibers," *Mechanics and Material Engineering for Science and Experiments*, 2003, pp. 172-175.

16. Yao, W.; Chen, B.; and Wu, K., "Smart Behavior of Carbon Fiber Reinforced Cement-Based Composite," *Journal of Materials Science and Technology*, V. 19, No. 3, 2003, pp. 239-243.

17. Bontea, D.-M.; Chung, D. D. L.; and Lee, G. C., "Damage in Carbon Fiber Reinforced Concrete, Monitored by Electrical Resistance Measurement," *Cement and Concrete Research*, V. 30, No. 4, 2000, pp. 651-659.

18. Fu, X., and Chung, D. D. L., "Self-Monitoring of Fatigue Damage in Carbon Fiber Reinforced Cement," *Cement and Concrete Research*, V. 26, No. 1, 1996, pp. 15-20.

19. Chung, D. D. L., "Damage in Cement-Based Materials, Studied by Electrical Resistance Measurement," *Materials Science and Engineering*, V. 42, No. 1, 2003, pp. 1-40.

20. Wen, S., and Chung, D. D. L., "Effects of Strain and Damage on the Strain Sensing Ability of Carbon Fiber Cement," *Journal of Materials in Civil Engineering*, V. 18, No. 3, 2006, pp. 355-360.

21. Wen, S., and Chung, D. D. L., "Self-Sensing of Flexural Damage and Strain in Carbon Fiber Reinforced Cement and Effect of Embedded Steel Reinforcing Bars," *Carbon*, V. 44, No. 8, 2006, pp. 1496-1502.

22. Chung, D. D. L., "Dispersion of Short Fibers in Cement," *Journal of Materials in Civil Engineering*, V. 17, No. 4, 2005, pp. 379-383.

23. Chen, B.; Wu, K.; and Yao, W., "Piezoresistivity in Carbon Fiber Reinforced Cement Based Composites," *Journal of Materials Science and Technology*, V. 20, No. 6, 2004, pp. 746-750.

24. Guan, X.; Han, B.; and Ou, J.-P., "The Mechanism and Some Properties of Carbon Fiber Reinforced Cement Sensor," *Advanced Smart Materials and Smart Structures Technology*, International Workshop, Honolulu, Hawaii, 2004, pp. 677-683.

25. Chen, B.; Wu, K.; and Yao, W., "Conductivity of Carbon Fiber Reinforced Cement-Based Composites," *Cement and Concrete Composites*, V. 26, 2004, pp. 291-297.

26. Wang, X.; Wang, Y.; and Jin, Z., "Electrical Conductivity Characterization and Variation of Carbon Fiber Reinforced Cement Composite," *Journal of Materials Science*, V. 37, No. 1, 2002, pp. 223-227.

27. Wu, B.; Huang, X.; and Lu, J., "Biaxial Compression in Carbon-Fiber-Reinforced Mortar, Sensed by Electrical Resistance Measurement," *Cement and Concrete Research*, V. 35, 2005, pp. 1430-1434.

28. Wu, K.; Chen, B.; and Yao, W., "Smart Properties of Carbon Fiber Reinforced Cement Based Composite," *Journal of Tonji University*, V. 30, No. 4, 2002, pp. 456-463.

29. Yao, W.; Chen, B.; and Wu, K., "Study of Smart Characteristics of Carbon Fiber Reinforced Cement-Based Materials," *Acta Materiae Compositae Sinica*, V. 19, No. 2, 2002, pp. 49-53.

30. Mao, Q.; Zhao, B.; Sheng, D.; Yang, Y.; and Shui, Z., "Resistance Changement of Compression Sensible Cement Specimen Under Different Stresses," *Workshop on Smart Materials*, Chinese National Natural Science Foundation, 1995, pp. 35-39.

31. Wen, S., and Chung, D. D. L., "The Role of Electronic and Ionic Conduction in the Electrical Conductivity of Carbon Fiber Reinforced Cement," *Carbon*, V. 44, No. 11, 2006, pp. 2130-2138.

32. Zhu, S., and Chung, D. D. L., "Numerical Assessment of the Methods of Measurement of the Electrical Resistance in Carbon Fiber Reinforced Cement," *Smart Materials and Structures*, in press.